MIDDLE-INFRARED PRISM SPECTROMETER FOR SINGLE-SHOT BUNCH LENGTH DIAGNOSTICS AT THE LCLS*

T. Maxwell[†], Y. Ding, A.S. Fisher, J. Frisch, H. Loos
SLAC National Accelerator Laboratory, Menlo Park, CA 94025, USA
C. Behrens, Deutsches Elektronen-Synchrotron, Hamburg, Germany

Abstract

Modern high-brightness accelerators such as laser plasma wakefield and free-electron lasers continue the drive to ever-shorter bunches. At low-charge (< 20 pC), bunches as short as 10 fs are reported at the Linac Coherent Light Source (LCLS) [1]. Advanced time-resolved diagnostics approaching the fs-level have been proposed requiring the support of rf-deflectors [2–4], modern laser systems, or other complex systems. Though suffering from a loss of phase information, spectral diagnostics remain appealing by comparison as compact, low-cost systems suitable for deployment in beam dynamics studies and operations instrumentation. Progress in mid-IR imaging and detection of the corresponding micrometer-range power spectrum has led to the continuing development of a single-shot, 1.2 - 40 micrometer prism spectrometer for ultra-short bunch length monitoring. In this paper we report further analysis and experimental progress on the spectrometer installation at LCLS [5].

INTRODUCTION

In low-charge mode, the LCLS FEL linac produces 13.6 GeV electron bunches with lengths on the order of a few micrometers and transverse spot size of ~50 μm [1] for delivery to the undulator hall to generate x-ray FEL pulses of comparable duration. Diagnosis of the longitudinal distribution at the undulator entrance is desired for FEL optimization studies and presents a unique challenge to the resolution of existing diagnostics, reaching into the 1-fs scale. Time-domain measurements of the LCLS beam by use of an x-band transverse deflecting-mode cavity are already being pursued [2–4]. Alternative frequency-domain diagnostics have advantages of economy, requiring only stand-alone optics capable of recording the spectrum of coherent beam radiation (CxR).

Under a change in trajectory or medium, the beam will radiate. In the 1-D line-charge approximation and neglecting other transverse effects, the radiation emitted will have a power spectrum that's given by

$$I(k) \propto I_e(k) \left[N + N(N - 1) \left| f(k) \right|^2 \right]$$ (1)

where $I_e(k)$ is the power spectrum for an individual electron in the given process, N is the number of electrons,

the "form factor" $f(k)$ is the Fourier transform of unit-normalized longitudinal charge distribution $\rho(z)$, and the wavenumber is defined as $k \equiv 1/\lambda$ (the spatial frequency).

The second term in the bracketed sum of Eq. (1) represents the CxR, having an additional factor N enhancement over the incoherent radiation over wavelengths corresponding to a large form factor. With a measurement of the beam spectrum in the region where the coherent spectrum falls off, one can then in principle deduce the bunch length. As a rule of thumb for the coherent cut-off wavelength, we consider a bunch with unit-normalized Gaussian distribution of rms length σ_z. In this case the corresponding form factor-squared $|f(k)|^2$ is also a Gaussian of frequency-independent peak amplitude that falls to 50% at the cut-offs

$$k_{50\%} = \frac{\sqrt{\ln 2}}{2\pi\sigma_z} \approx \frac{0.133}{\sigma_z} \Rightarrow \lambda_{50\%} \approx 7.55\sigma_z$$ (2)

Prior LCLS studies on low-charge operation suggest bunch length scaling linearly with charge at a constant peak current [1]. For $Q = 10 - 200$ pC, we have $\sigma_z = 0.5 - 50$ μm for typical bunch compression. This yields coherent enhancement down to $\lambda = 3.5 - 40$ μm (up to $k = 2900$-250 cm^{-1}).

As the distribution of the LCLS beam can vary from shot-to-shot, traditional scanning THz interferometry methods are avoided in favor of a single-shot mid-IR spectrometer inspired by that demonstrated in [6]. Here we provide an update on a one-stage, Single-Shot THz Prism Spectrometer (SSTPS) installation designed to cover this spectral range [5], favoring compactness and simplicity.

SYSTEM OVERVIEW

Current LCLS relative bunch length monitors utilize the coherent edge radiation (CER) emitted at the exit of upstream bending magnets [7]. For the present application in the straight section of the LCLS beam transport hall, coherent transition radiation (CTR) from the beam impinging on an inserted foil [8] was chosen. Referring to the overview for the SSTPS system in Fig. 1, light from the foil (A) will be collected and focused onto the spectrometer slit (F). Light at the slit is collimated through a custom KRS-5 mid-IR prism to provide dispersion (H) before being focused onto a linear pyroelectric detector array (J). All-reflective imaging optics are used to avoid unwanted chromatic abberations. The system is considered in two parts: the light collection optics (A-F) and the spectrometer proper (F-J).
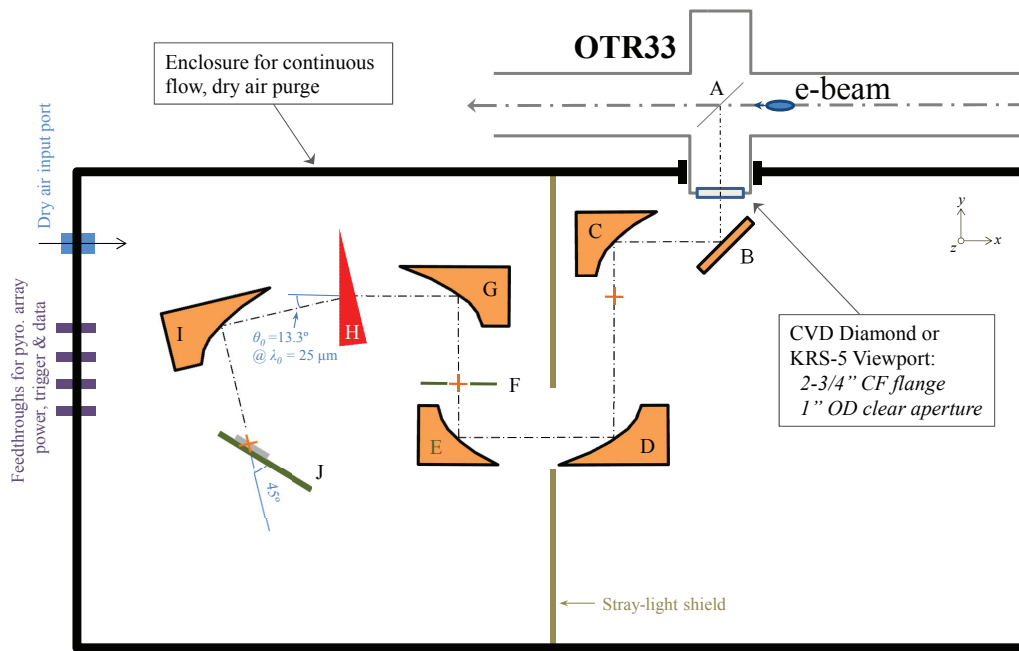
Figure 1: Schematic of SSTPS to be installed at LCLS diagnostic cross OTR33, just prior to the undulator hall. CTR from a thin foil inserted into the beam (A) is collected and imaged to the spectrometer slit (B-F) and spectrally resolved on the detector (F-J) using a custom KRS-5 mid-IR prism as the dispersive element (H).

Design of the system is dictated by maintaining high, flat light transmission over the one to tens of micron wavelength band. For coupling the light out of the vacuum pipe, both CVD diamond and KRS-5 viewports are available with transmission spectra shown in Fig. 2. KRS-5 shows very flat transmission over the full 1-40 μm (250-8000 cm^{-1}) range, but is brittle and slightly hygroscopic. CVD diamond will be used for initial tests despite known phonon absorption lines at 2 and 6 μm.

Also shown in Fig. 2 is the transmission spectrum through 1 m of ambient air [9]. Several absorption bands are seen from the presence of water vapor. These can be improved to the better than 90% level with an 80% reduction in relative humidity. A dry-air purged enclosure has therefore been designed with the added benefit of protecting any slightly hygroscopic optics.

Light Collection and Alignment

Collection optics require consideration of the CTR source. Transition radiation is highly directional, concentrated on a cone with half-apex angle $1/\gamma$ in the far field [8]. The light must pass the narrow aperture (100 μm) slit.

For these reasons, and to further discriminate against incoherent transition radiation by its larger inherent divergence, an odd number of "lenses" is used to provide wide spatial acceptance and narrow angular acceptance. By ray trace design, light from the foil within $\Delta x = \pm 7.2$ mm will clear the slit but only within $\Delta \theta_x = \pm 0.2°$.

The LCLS is a user-oriented facility with minimal downtime. Therefore the entire 2'×4' breadboard has been de-
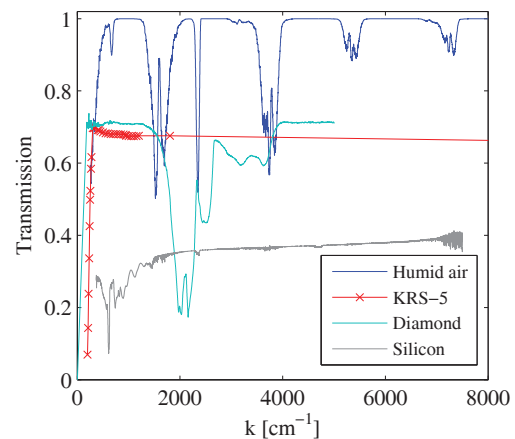

Figure 2: Transmission function of various substances in spectral range of interest.

signed for rapid installation and removal. The table mount (Fig. 3) is a quick-release, turn-buckle design so that the board can be positioned and aligned within the required tolerance. The initial turning mirror (Fig. 1, B) is used for fine angular control to position the image on the slit, and remotely as necessary. The board can be locked to a table in an offline optics lab for preparation and testing.

To get initial alignment, a reference alignment laser will be added during installation. A new 6-way cross 7.3 m upstream of OTR33 will inject the laser into the beam line, imaged to match the noted beam position on the existing OTR33 camera. With reference positioned to within
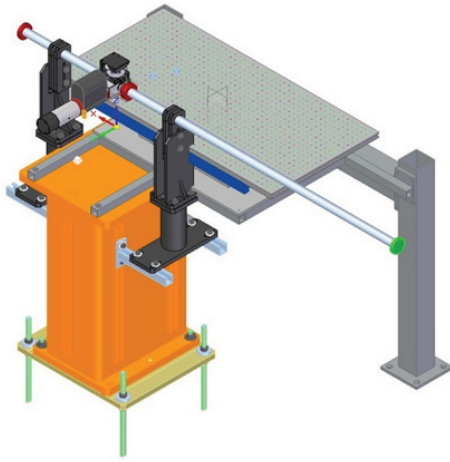
Figure 3: Rendering of the new OTR33 diagnostic station. SSTPS optics and enclosure to be installed on the quick-release breadboard.

±2 mm of the beam center at both crosses, the angle is restricted to within ±0.03° and well within the stated acceptance of the system.

The Spectrometer

A prism spectrometer configuration was chosen as a matter of simplicity and economy, though order-sorted grating configurations have gains in resolution [5, 6]. Chosen for its broad mid-IR transmission (Fig. 2) and moderate dispersion, KRS-5 was chosen as the prism medium [5] with index and dispersion curves shown in Fig. 4. Using the 12.8 mm length of the detector array as a restriction to the maximum spatial dispersion, the prism apex angle is 10°.

Figure 4 shows nonlinearity over this wide spectral range. With a constant waist of 10-mm at the prism, the frequency-to-position map $x(k)$ and effective spectral resolution $\Delta k(k)$ is computed in Fig. 5. While the strong low-k dispersion and small diffraction-limited spots at high-k
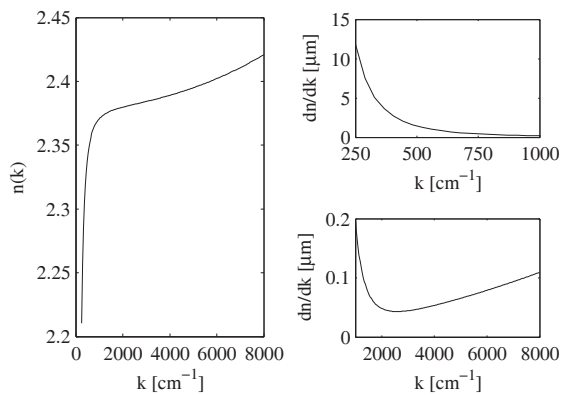

Figure 4: Refractive index $n(k)$ (left) and dispersion $n'(k)$ (right) for KRS-5.
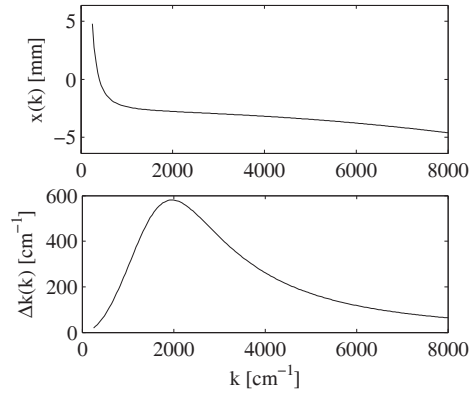

Figure 5: Frequency dependence of spectral spot positions $x(k)$ (top) and spectral resolution $\Delta k(k)$ (bottom) for prism spectrometer (Fig. 1).

preserve good spectral resolution in these limits, the center band about $k = 2000$ cm^{-1} suffers. The strong frequency dependence of $x(k)$ also suggests that excellent wavelength calibration is required.

ABSOLUTE LEVELS

To compare expected light levels as compared to detector sensitivity and to quantify the extent of information loss in the system, additional modeling and testing was performed. These include analysis of transverse imaging contributions, detector benchmarking and absolute power estimations.

Transverse Contributions

Considerable work has been done on modeling the generation and diffraction of near-field, long-wavelength CTR in recent years and is known to cause significant low-frequency losses. This was modeled for the SSTPS using [10] following the approach outlined in [7]. Diffraction of light through the system is accomplished by Gauss-Laguerre mode decomposition of the fields between apertures [11]. The finite TR source is estimated by the method of virtual quanta [12] as the Fourier components of the relativistic single-electron fields diffracting through the OTR screen.

The full system was optimized with results in Fig. 6. Significant low-k losses are observed arising primarily at the spectrometer slit (Fig. 1, F). The 3-lens imaging was chosen to prefer spatial acceptance and also improves peak system transmission shown here. However this choice gives rise to the strong DC suppression and long rise in response due to the frequency dependence of the divergence of the diffracted, near-field TR.

Detector Sensitivity

The 128-element, linear pyroelectric array being used is provided by Pyreos [13]. Pixels are 60 μm wide and 500 μm tall with a 100 μm pitch. The manufacturer also
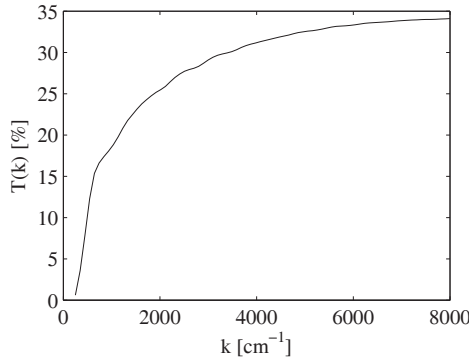
Figure 6: Simulated CTR diffraction losses for the SSTPS system.

Figure 8: Line array signal from focused 3.4-μm HeNe synchronously chopped to 85 μs pulse width at 100 Hz.

furnishes a compact data acquisition board for the sensor. The kit generates the timing signals required by the sensor and digitizes the analog burst with a sampling rate of ν_{samp} = 10 - 256 Hz. The sensor and kit are shown in Fig. 7.

As previously reported [5], the sensitivity is not provided. It has since also been noted that the sensor array contains unpassivated silicon. To prevent disrupting photoelectron emission within the detector circuit, a low-pass optical filter must block $\lambda < 1.2$ μm. A silicon window is being used along with the acquisition kit. Measured mid-IR silicon transmission is shown in Fig. 2 [14], and is strongly attenuating in the visible to near IR.

Illumination tests were repeated using a 2-mW, 3.4-μm HeNe laser. The beam is first combined with a visible 632 nm HeNe laser by transmission (reflection) of the IR (visible) beam through a germanium combiner. The beams are then chopped and reflectively expanded. A silicon photodiode is used to check time of arrival of the laser pulse(s) and estimate the variable chopped IR pulse width τ_{pulse}. When $\tau_{pulse} \ll 1/(2\nu_{samp})$, the optimal array signal coincides with the kit triggered just after termination of the light pulse.

The beam is focused to a tight spot on the array with an example image from a 100-Hz, 85-μs (fwhm) chopped pulse shown in Fig. 8. From such data, and accounting for 48% transmission of the 2-mW IR laser through the Ge combiner, the sensitivity of the array (with window) is es-
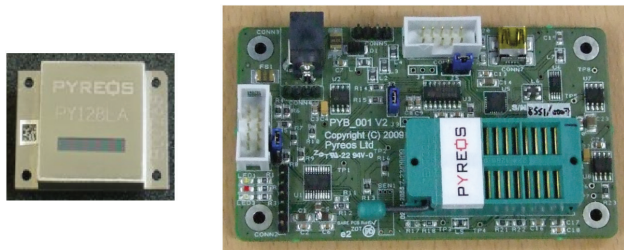
timated to be 75 V/μJ/pixel. With saturation occurring at 4.5 V, maximum illumination is around 60 nJ/pixel. Averaging over many shots, rms electrical noise is 15 mV/pixel. This corresponds to a lower limit of 0.2 nJ/pixel.

Simulated Signal

Finally we illustrate expected signals for low-charge operation of the LCLS linac. A simulated bunch distribution for the typical under- to fully-compressed, double-horn bunch [1] is used. Assuming still a constant peak current and that bunch duration scales with charge, simulated initial distributions and spectra are shown in Fig. 9.

To simulate measured signals, the spectra are subjected to losses (Fig. 6), mapped to detector position (Fig. 5, top), convolved with a resolution term (Fig. 5, bottom), integrated over the region subtended by each pixel, and summed with psuedo-electrical noise of amplitude 0.5 nJ/pixel. The results are shown in Figs. 10 and 11 for the 200- and 20-pC cases, respectively.

By these estimates, the single-bunch light levels fall within the range of the sensor. For the 200-pC (10's of μm) case, there is a loss of amplitude definition as the edge of the spectrum falls within the low-resolution range (Fig. 5).

Figure 7: The 128-element linear pyroelectric array (left) and data acquisition evaluation kit (right). Images courtesy of Pyreos [13, 15].
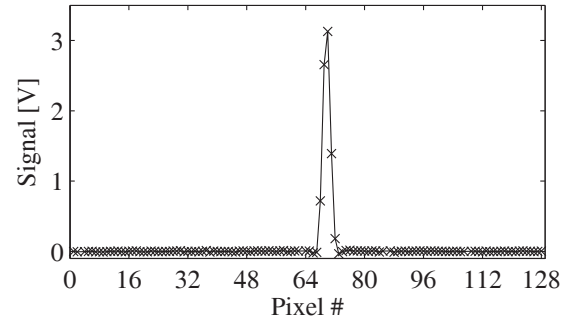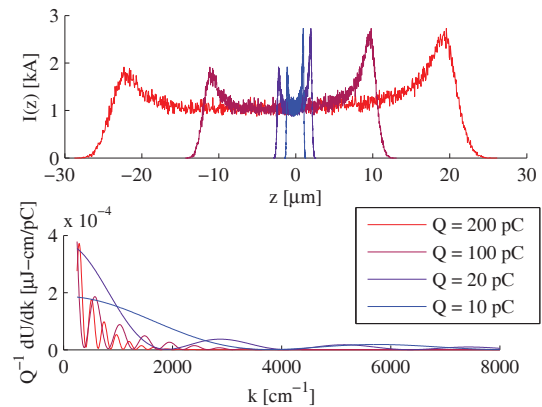

Figure 9: Simulated bunch profiles (top) and corresponding emitted power spectra per unit charge (bottom).
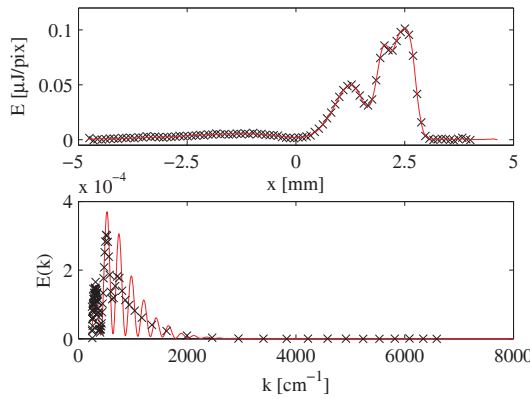
Figure 10: Simulated detector array levels before (top) and after (bottom) mapping to k axis for $Q = 200$ pC case.
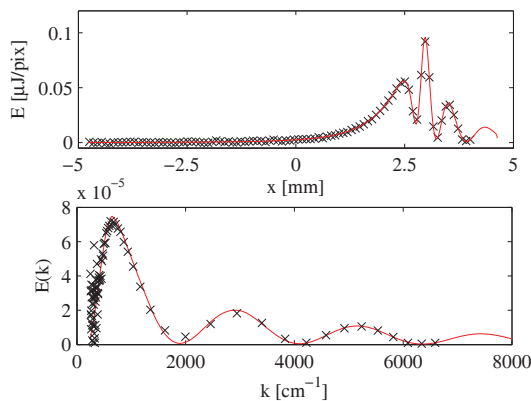

Figure 11: Simulated detector array levels before (top) and after (bottom) mapping to k axis for $Q = 20$ pC case.

Simulations around 20 pC prove more promising with significant structure of the spectrum preserved.

DISCUSSION

Progress continues on a Single-Shot, THz Prism Spectrometer for absolute, ultra-short bunch length diagnostics at the LCLS. Rigorous simulations of the system have been carried out with the novel detector's behavior and control now well understood. Practical installation issues have been addressed.

Staging of the final optics and electronics is nearly complete. In parallel with the ongoing fabrication of various necessary mounting components, plans for improved spectrometer characterization are underway. These will use the LCLS Laser Group's micron-range OPA and monochromator to provide a wavelength calibration measurement.

The projected instrument response suggests optimal operation is in the 10's of pC range, with bunches of a few-μm length. Though spectral methods do not directly deduce absolute bunch length due to loss of phase information, simulated signals in this range have also proven amenable to

Kramers-Kronig phase retrieval [16] after all expected distortions, demonstrating promise as an absolute diagnostic in support of LCLS ultra-short FEL optimization studies on track for first beam measurements before end of calendar year.

REFERENCES

[1] Y. Ding et al., Phys. Rev. Lett. **102**, 254801 (2009).

[2] P. Emma, J. Frisch, and P. Krejcik, *A Transverse RF Deflecting Structure for Bunch Length and Phase Space Diagnostics*, SLAC Technical Note LCLS-TN-00-12 (2000).

[3] Y. Ding et al., Phys. Rev. ST Accel. Beams **14**, 120701 (2011).

[4] P. Krejcik et al., Proc. of IBIC2012, TUPA41 (2012).

[5] C. Behrens et al., Proc. of DIPAC2011 pp. 386–388 (2011).

[6] S. Wesch et al., Nucl. Instr. Meth. A **665**, 40 (2011).

[7] H. Loos et al., Proc. of PAC07 pp. 4189–4191 (2007).

[8] V. Ginzburg and I. Frank, J. Phys. USSR p. 353 (1945).

[9] Harvard-Smithsonian Cen. for Astro. and V.E. Inst. of Atmos. Opt., *HITRAN Database*, Available at HITRAN on the Web: `http://hitran.iao.ru` (2012).

[10] H. Loos, *CxR Simulation Tool*, SLAC MATLAB code `spec_gui.m` (2010).

[11] H. Kogelnik and T. Li, Proc. IEEE p. 1312 (1966).

[12] C. A. Brau, *Modern Problems in Classical Electrodynamics* (Oxford University Press, New York, 2004).

[13] Pyreos Ltd., *PY-LA-S-128 Product Datasheet*, Available at `http://www.pyreos.com/images/docs/PY-LA-S-128_May2010finalrelease.pdf` (2010).

[14] Tydex, Russia, *private communication* (2012).

[15] Pyreos Ltd., *Line Sensor Evaluation Kit Product Datasheet*, Available at `http://www.pyreos.com/images/docs/PYDK_LAS_Demo_Kit_User_Guide__JWrelease_Jan2010.pdf` (2010).

[16] R. Lai and A. Sievers, Nucl. Instr. Meth. A **397**, 221 (1997).